Gamma Interactions: Photoelectric Effect and Pair Production

References:

R. D. Evans, Atomic Nucleus (McGraw-Hill New York, 1955), Chaps 24, 25.

W. E. Meyerhof, *Elements of Nuclear Physics* (McGraw-Hill, New York, 1967), pp. 91-108.

W. Heitler, *Quantum Theory of Radiation* (Oxford, 1955), Sec. 26.

Photoelectric Effect

This is the predominant mode of γ - interaction in all kinds of matter, especially the high-Z absorbers, at energies less than ~ 0.1 Mev. The process, sketched in Fig. 18. 1, is the interaction between the gamma and the entire atom (the electron cloud) that results in the absorption of the gamma and the ejection of an electron with kinetic energy

$$T \sim \hbar\omega - B_e \qquad (18.1)$$

where B_e is the electron binding energy. The recoiling atom is left in an excited state at an excitation energy of B_e; it can then de-excite by emitting x-rays or Auger electrons.
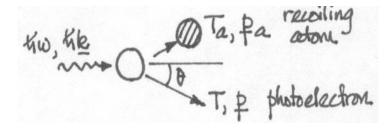

Fig. 18.1. Schematic of photoelectric effect, absorption of an incident gamma ray and the ejection of an atomic electron and excitation of the recoiling atom.

Notice this is atomic and not nuclear excitation. One can show that the incident γ cannot be totally absorbed by a free electron because momentum and energy conservations cannot be satisfied simultaneously, but total absorption can occur if the electron is initially bound in an atom. The most tightly bound electrons have the greatest probability of absorbing the γ. It is known theoretically and experimentally that $\sim 80\%$ of the absorption occurs in the K (innermost) shell, so long as $\hbar\omega > B_e(K-shell)$. Typical ionization potentials of K electrons are 2.3 kev ($A\ell$), 10 kev (Cu), and ~ 100 kev (Pb).

The conservations equations for photoelectric effect are

$$\hbar\underline{k} = \underline{p} + \underline{p}_a \tag{18.2}$$

$$\hbar\omega = T + T_a + B_e \tag{18.3}$$

where $\underline{p}_a$ is the momentum of the recoiling atom whose kinetic energy is T_a. Since $T_a \sim T(m_e/M)$, where M is the mass of the atom, one can usually ignore T_a.

The theory describing the photoelectric effect is essentially a first-order perturbation theory calculation (cf. Heitler, Sec. 21). In this case the transition taking place is between an initial state consisting of two particles, a bound electron, wave function $\sim e^{-r/a}$, with $a = a_o/Z$, a_o being the Bohr radius ($= \hbar^2/m_e e^2 = 0.529 \times 10^{-8}$ cm), and an incident photon, wave function $e^{i\underline{k}\cdot\underline{r}}$, and a final state consisting of a free electron whose wave function is $e^{i\underline{p}\cdot\underline{r}/\hbar}$. The interaction potential is of the form $\underline{A}\cdot\underline{p}$, where A is the vector potential of the electromagnetic radiation and $\underline{p}$ is the electron momentum. The result of this calculation is

$$\frac{d\sigma_\tau}{d\Omega} = 4\sqrt{2}\frac{r_e^2 Z^5}{(137)^4}\left(\frac{m_e c^2}{\hbar\omega}\right)^{7/2}\frac{\sin^2\theta\cos^2\varphi}{\left(1-\frac{v}{c}\cos\theta\right)^4} \tag{18.4}$$

where v is the photoelectron speed. The polar and azimuthal angles specifying the direction of the photoelectron are defined in Fig. 18.2. One should pay particular notice to the Z^5 and $(\hbar\omega)^{-7/2}$ variation. As for the angular dependence, the numerator in
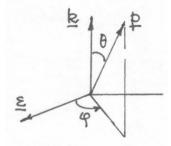

Fig. 18.2. Spherical coordinates defining the photoelectron direction of emission relative to the incoming photon wave vector and its polarization vector.

(18.4) suggests an origin in $(p \cdot \varepsilon)^2$, while the denominator suggests $p \cdot k$. Integration of (18.4) gives the total cross section

$$\sigma_\tau = \int d\Omega \frac{d\sigma_\tau}{d\Omega} = 4\sqrt{2}\sigma^o \frac{Z^5}{(137)^4}\left(\frac{m_e c^2}{\hbar\omega}\right)^{7/2} \tag{18.5}$$

where one has ignored the angular dependence in the denominator and has multiplied the result by a factor of 2 to account for 2 electrons in the K-shell [Heitler, p. 207].

In practice it has been found that the charge and energy dependence behave more like

$$\sigma_\tau \propto Z^n /(\hbar\omega)^3 \tag{18.6}$$

with n varying from 4 to 4.6 as $\hbar\omega$ varies from ~ 0.1 to 3 Mev, and with the energy exponent decreasing from 3 to 1 when $\hbar\omega \geq m_e c^2$. The qualitative behavior of the photoelectric cross section is illustrated in the figures below.
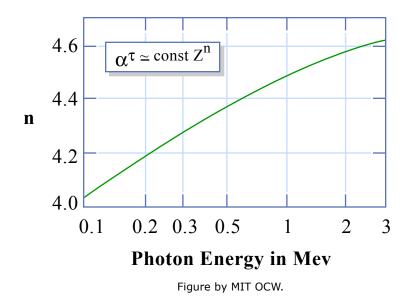
Figure by MIT OCW.

Fig. 18.3. Variation with energy of incident photon of the exponent n in the total cross section for photoelectric effect. (from Evans)
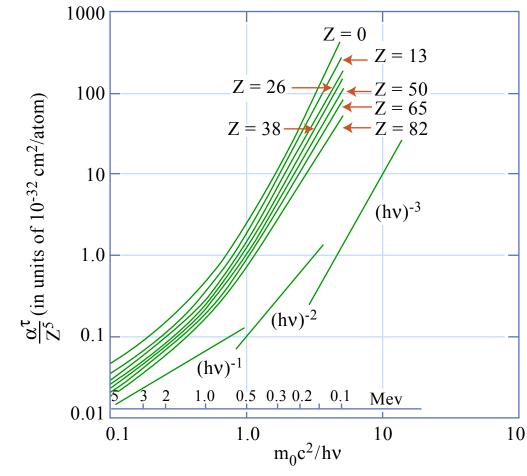

Figure by MIT OCW.

Fig. 18.4. Photoelectric cross sections showing approximate inverse power-law behavior which varies with the energy of the incident photon. (from Evans)
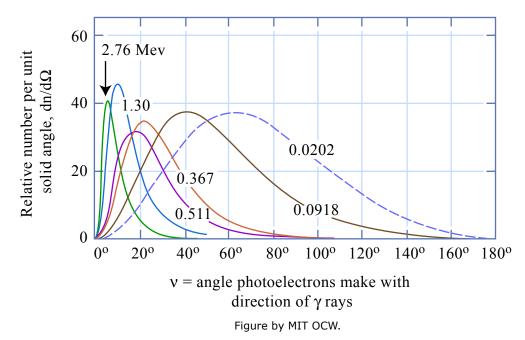
Figure by MIT OCW.

Fig. 18.5. Angular distribution of photoelectrons for various incident photon energies. The peak moves toward forward direction as the energy increases, a behavior which can be qualitatively obtained from the θ-dependence in Eq. (18.4). (from Meyerhof)

Edge Absorption

As the photon energy increases the cross section σ_{κ} can show discontinuous jumps which are known as *edges*. These correspond to the onset of additional contributions when the energy is sufficient to eject an inner shell electron. The effect is more pronounced in the high-Z material. See Fig. 18.13 below.

Pair Production

In this process, which can occur only when the energy of the incident γ exceeds 1.02 Mev, the photon is absorbed in the vicinity of the nucleus, a positron-electron pair is produced, and the atom is left in an excited state, as indicated in Fig. 18.6. The
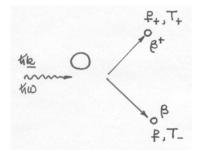

Fig. 18.6. Kinematics of pair production.

5

conservation equations are therefore

$$\hbar\underline{k} = \underline{p}_+ + \underline{p}_-$$ (18.7)

$$\hbar\omega = \left(T_+ - m_e c^2\right) + \left(T_- + m_e c^2\right)$$ (18.8)

One can show that these conditions cannot be satisfied simultaneously, the presence of an atomic nucleus is required. Since the nucleus takes up some momentum, it also takes up some energy in the form of recoil.

The existence of positron is a consequence of the Dirac's relativistic theory of the electron which allows for negative energy states,

$$E = \pm\left(c^2 p^2 + m_e^2 c^4\right)^{1/2}$$ (18.9)

One assumes that all the negative states are filled; these represent a "sea" of electrons which are generally not observable because no transitions into these states can occur due to the Exclusion Principle. When one of the electrons makes a transition to a positive energy level, it leaves a "hole" (positron) which behaves likes an electron but with a *positive* charge. This is illustrated in Fig. 18.7. In other words, holes in the
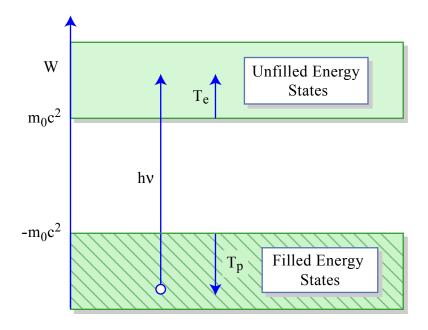

Figure by MIT OCW.

Fig. 18.7. Creation of a positron as a "hole" in the filled (negative) energy states and an electron as a particle in the unfilled energy state. (from Meyerhof)

negative energy states have positive charge, whereas an electrons in the positive energy states have negative charge. The "hole" is unstable in that it will recombine with an electron when it loses most of its kinetic energy (thermalized). This recombination process is called pair annihilation. It usually produces two γ (annihilation radiation), each of energy 0.511 Mev, emitted back-to-back. A positron and an electron can form an atom called the positronium. It's life time is $\sim 10^{-7}$ to 10^{-9} sec depending on the relative spin orientation, the shorter lifetime corresponding to antiparallel orientation.

Pair production is intimately related to the process of *Bremsstrahlung* in which an electron undergoes a transition from one positive energy state to another while a photon is emitted. One can take over directly the theory of *Bremsstrahlung* for the transition probability with the incident particle being a photon instead of an electron and using the appropriate density of states for the emission of the positron-electron pair [Heitler, Sec. 26]. For the positron the energy differential cross section is

$$\frac{d\sigma_\kappa}{dT_+} = 4\sigma_o Z^2 \frac{T_+^2 + T_-^2 - \frac{2}{3}T_+T_-}{(\hbar\omega)^3}\left[\ell n\left(\frac{2T_+T_-}{\hbar\omega m_e c^2}\right) - \frac{1}{2}\right] \qquad (18.10)$$

where $\sigma_o = r_e^2/137 = 5.8 \times 10^{-4}$ barns. This result holds under the conditions of Born approximation, which is a high-energy condition ($Ze^2/\hbar v_+ \ll 1$), and no screening, which requires $2T_+T_-/\hbar\omega m_e c^2 \ll 137/Z^{1/3}$. Here screening means the partial reduction of the nuclear charge by the potential of the inner-shell electrons. As a result of the Born approximation, the cross section is symmetric in T_+ and T_-. Screening effects will lead to a lower cross section.

To see the energy distribution we rewrite (18.10) as

$$\frac{d\sigma_\kappa}{dT_+} = \frac{\sigma_o Z^2}{\hbar\omega - 2m_e c^2}P \qquad (18.11)$$

where the dimensionless factor P is a rather complicated function of $\hbar\omega$ and Z; its behavior is depicted in Fig. 18.8. We see the cross section increases with increasing
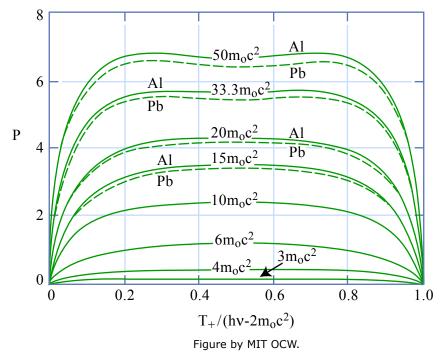

Figure by MIT OCW.

Fig. 18.8. Calculated energy distribution of positron emitted in pair production, as expressed in Eq.(18.11), with correction for screening (dashed curves) for photon energies above $10m_ec^2$. (from Evans)

energy of the incident photon. Since the value is slightly higher for Al than for Pb, it means the cross section varies with Z somewhat weaker than Z^2. At lower energies the cross section favors equal distribution of energy between the positron and the electron, while at high energies a slight tendency toward unequal distribution could be noted. Intuitively we expect the energy distribution to be biased toward more energy for the positron than for the electron simply because of Coulomb repulsion of the positron and attraction of the electron by the nucleus.

The total cross section for pair production is obtained by integrating (18.11). Analytical integration is possible only for extremely relativistic cases [Evans, p. 705],

$$\sigma_\kappa = \int dT_+ \left(\frac{d\sigma_\kappa}{dT_+} \right) = \sigma_o Z^2 \left[\frac{28}{9} \ell n \left(\frac{2\hbar\omega}{m_ec^2} \right) - \frac{218}{27} \right], \quad \text{no screening} \qquad (18.12)$$

$$= \sigma_o Z^2 \left[\frac{28}{9} \ell n \left(\frac{183}{Z^{1/3}} \right) - \frac{2}{27} \right], \quad \text{complete screening} \qquad (18.13)$$

Moreover, (18.12) and (18.13) are valid only for $m_e c^2 \ll \hbar \omega \ll 137 m_e c^2 Z^{-1/2}$ and

$\hbar \omega \gg 137 m_e c^2 Z^{-1/2}$ respectively. The behavior of this cross section is shown in Fig. 18.9, along with the cross section for Compton scattering. Notice that screening leads to a saturation effect (energy independence); however, it is not significant below $\hbar \omega \sim 10$ Mev
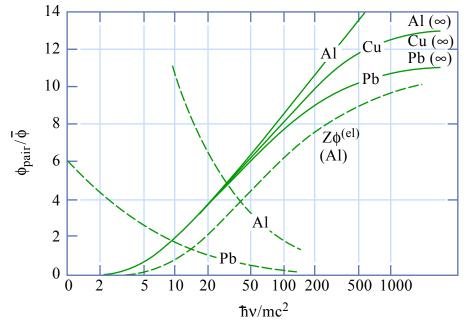

Figure by MIT OCW.

Fig. 18.9. Energy variation of pair production cross section in units of $\sigma_o Z^2$.

Mass Attenuation Coefficients

So long as the different processes of photon interaction are not correlated, the total linear attenuation coefficient μ for γ-interaction can be taken as the sum of contributions from Compton scattering, photoelectric effect, and pair production, with $\mu = N\sigma$ and N being the number of atoms per cm3. Since $N = N_o \rho / A$, where N_o is Avogardro's number and ρ the mass density of the absorber, it is again useful to express the interaction in terms of the *mass attenuation coefficient μ / ρ*. As we had discussed in Lecture 14, this quantity is essentially independent of the density and physical state of the absorber. Recall our observation in the case of charged particle interactions that Z/A is approximately constant for all elements. Here we see that in the product $N\sigma$ we get a factor of 1/A from N, and we can get a factor of Z from any of the three cross sections σ, so we can also take advantage of Z/A being roughly constant in describing photon

interaction (the same argument does not hold for neutrons even though it is useful to think of neutron interactions in terms of the macroscopic cross section Σ). We write

$$\mu = \mu_C + \mu_\tau + \mu_\kappa \tag{18.14}$$

$$\mu_C / \rho = (N_o / A)Z\sigma_C, \quad \sigma_C \sim 1/\hbar\omega \qquad \text{per electron} \tag{18.15}$$

$$\mu_\tau / \rho = (N_o / A)\sigma_\tau, \qquad \sigma_\tau \sim Z^5 /(\hbar\omega)^{7/2} \qquad \text{per atom} \tag{18.16}$$

$$\mu_\kappa / \rho = (N_o / A)\sigma_\kappa, \qquad \sigma_\kappa \sim Z^2 \ell n(2\hbar\omega / m_e c^2) \quad \text{per atom} \tag{18.17}$$

It should be quite clear by now that the three processes we have studied are not equally important for a given region of Z and $\hbar\omega$. Generally speaking, photoelectric effect is important at low energies and high Z, Compton scattering is important at intermediate energies ($\sim 1 - 5$ Mev) and all Z, and pair production becomes at higher energies and high Z. This is illustrated in Fig. 18.10.

We also show several mass attenuation coefficients in Figs. 18.11 – 18.13. One should make note of the magnitude of the attenuation coefficients, their energy dependence, and the contribution associated with each process. In comparing theory with experiment the agreement is good to about 3 % for all elements at $\hbar\omega < 10m_e c^2$. At higher energies disagreement sets in at high Z (can reach $\sim 10\%$ for Pb), which is due to the use Born approximation in calculating σ_κ. If one corrects for this, then agreement to within $\sim 1\%$ is obtained out to energies ~ 600 $m_e c^2$.
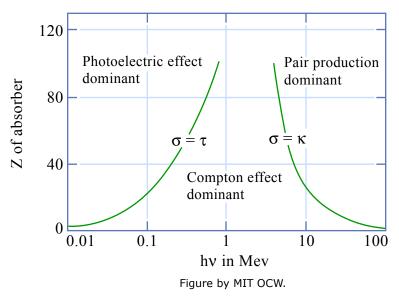
Figure by MIT OCW.

Fig. 18.10. Regions where one of the three γ-interactions dominates over the other two. (from Evans)
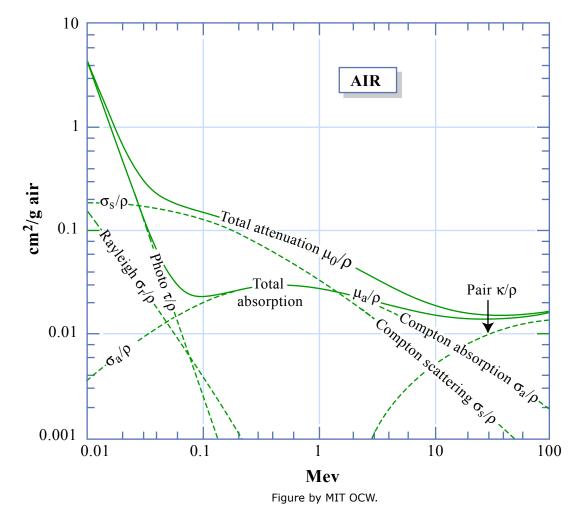

Figure by MIT OCW.

Fig. 18.11. Mass attenuation coefficient for photons in air computed from tables of atomic cross sections. (from Evans)
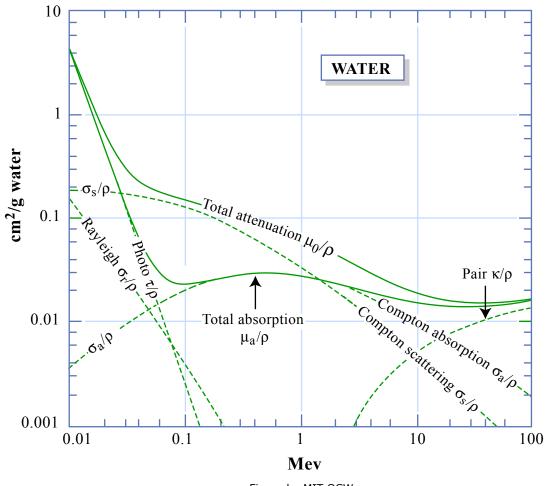
Figure by MIT OCW.

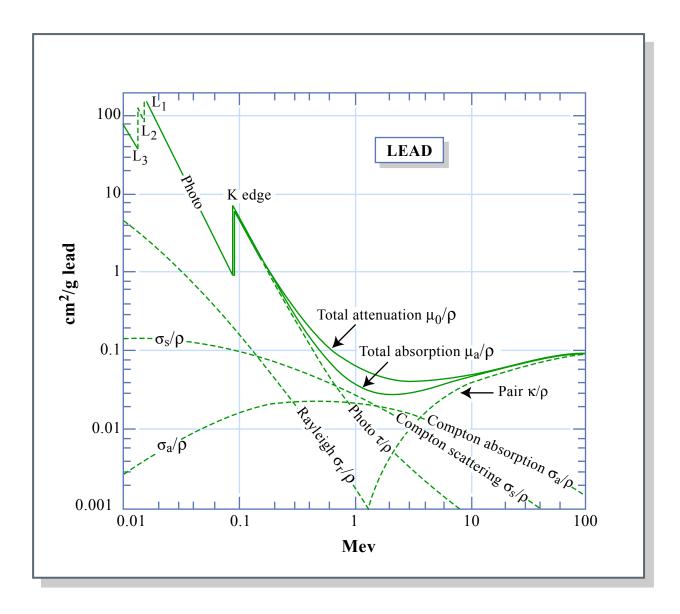**Fig. 18.12.** Mass attenuation coefficients for photons in water. (from Evans)

Figure by MIT OCW.

Fig. 18.13. Mass attenuation coefficients for photons in Pb. (from Evans)